Bioactivity and Flexural Strength of Orthopaedic Regenerative Mg AZ31 and Mg Zn 0.6Ca Alloys: In-vitro Study

Rehab Salah[1*], Hatem M. Ibrahim[2], Madiha M. Shoeib[3], Amr H. EI-Bolok[4], Heba A. Shalaby[5]

Abstract

Aim: Evaluating the bioactivity of orthopaedic Magnesium alloy and its flexural strength.(MgAZ31 and Mg1Zn0.6Ca Alloys).**Materials and Methods:** two types of alloys MgAZ31 and Mg1Zn0.6Ca were studied. Eighty rectangular rods for each tested alloy were prepared. Sixty rectangular rods were immersed in simulated body fluid (SBF) for different time intervals; two, four and 8weeks (n=10/each time interval). All tested groups were chemically analyzed qualitatively and quantitatively by using FTIR, and SEM with EDX.The mineral, hydroxyapatite crystal maturity, and degree of crystallinity were calculated to evaluate the amount of mineral formed. The amount of amide I and degree of calcification were calculated to evaluate the amount of matrix formed. All the calculated parameters were compared with normal bone. The flexural strength was measured before and after biomimetic immersion. **Results:** SEM with EDX of group I showed greater amount of loss in Mg, Al, and Zn elements from the surface of alloy more than Group IIB at all-time interval. HA crystal maturity and degree of HA crystallinity of group II were 77.9% and 20.6% from normal Cancellous bone after two weeks that decreased after four weeks to be 53.9% and 5.3% whereas after eight weeks increased again to be 161% and 65.5% from normal Cancellous bone. The amount of amide I was 0.008% for group I and the degree of calcification was 6.3%for group I after 2week. The flexural strength after two weeks for group IIB was recorded the highest value compared to group IB (130.67±0.03 and102.65±0.03) respectively. **Conclusions:** Mg1Zn0.6Ca enhanced the deposition of mature HA with better crystallinity and rational degree of calcification near normal bone in composition. Immersion of the Mg-alloy in SBF encouraged deposition of minerals with different quality rather than the matrix. Mg1Zn0.6Ca alloy revealed rational flexural strength which is superior than AZ31.

KeyWords: Mg-alloy, flexural strength, FTIR, SEM, EDX, Simulating body fluid, Biodegradable Mg-based alloy, Bioactivity.

DOI Number: 10.14704/NQ.2022.20.15.NQ88223 **NeuroQuantology2022;20(15):2357-2366**

*Correspondingauthor:Rehab Salah **E-mail:**Rehab.salah77@yahoo.com
Phone number: (+2) 01144258777; **Address:** Nahda University, new Beni-Suef city, Beni-Suef Government, Egypt.

Affiliations:

1. Assistant lecturer, Department of Dental Biomaterial, Faculty of Oral and Dental Medicine, Nahda University, Beni-Suef, Egypt.
2. Lecturer of Dental Biomaterials, College of Oral and Dental Medicine and Surgery, Misr University for Science and Technology (MUST), Egypt.
3. Professor, Former head of surface treatment and corrosion department (CMRDI), Egypt.
4. Professor of Oral Pathology and Head of Oral Pathology Department, Minia University, Egypt.
5. Associate Professor of Dental Biomaterial, Faculty of Oral and Dental Medicine, Nahda University, Beni-Suef, and Associate professor of Dental Biomaterial, Faculty Dentistry, Alfyoum University, Alfyoum, Egypt.

Relevant conflicts of interest/financial disclosures:
The authors declare that the research was conducted in the absence of any commercial or financial relationships that could be construed as a potential conflict of interest.

Introduction:

Magnesium alloys have been used as orthopedic biodegradable implants due to their good biocompatibility and close mechanical properties to natural bone (1). The elastic modulus of Mg alloys, about 45 GPa, is relatively close to that of natural bone (3–20 GPa) (2). Furthermore, second surgical intervention can be avoided(3).Pure Magnesium are extremely susceptible to corrosion in the physiological pH (7.4–7.6). Hydrogen gases are released in high amounts leading to impair defective bone healing and early rapid degradation. The early degradation leading to loss of the mechanical integrity of implant before complete healing (4). Hence pure Mg was alloyed with different elements to control the degradation rate and improved their strength(5). Zn, Ca, Zr, Mn,Al and Si are elements were added to Mg to improve their biocompatibility and Osseo integrative potentiality(6).

Magnesium–aluminum (Mg-Al) based alloys are used due to their excellent castability, accepted mechanical properties at room temperature, and good corrosion resistance. However, the mechanical properties of Mg-Al based alloys significantly decrease as the β- phases are precipitated at grain boundaries, Addition of Zn as an alloying element can refine the grain size and improve the corrosion resistance and mechanical properties of Mg –Al alloy(7)(8).

Zinc is one of the essential trace elements for the human body. It is crucial for many biological functions; for bone development, mineralization, and mass preservation (9).Addition of small amount of Zn (1 wt.%) improved the corrosion resistance and enhanced calcium phosphate deposition of Mg-Al based alloys as in AZ31 (10). It was found that a biocompatible Calcium phosphate protective film layer covers the surfaces of the AZ31 and AZ91 alloys, which stimulates the creation of new bone mass around the implants, according to short-term in vivo investigations of these materials (11)(12).

Calcium (Ca) is a key component of human bone. It promotes bone repair and crucial for bone cell signaling. It has the capacity to improve microstructure (13). Ca has been added to Mg-Zn based alloys have good potential to be high strength wrought magnesium alloys (14), due to their significant solution, and precipitation strengthening(15).Hence Mg1Zn 0.6Ca that contained calcium are promising alloy for bone regeneration(16).

Mg alloy should have an adequate mechanical fixation for bone defect so the biodegradation rate of Mg alloy should be synchronized with new bone formation. Mg alloy should have the ability to induce sufficient bone of high quality on its surface before the implant decomposes or losing its efficient (strength) (17).

Bioactivity of Mg can be measured by many in vitro methods as immersion in SBF, Cell Adhesion,Cell Proliferation and differentiation assays (UMSCs). The amount and quality of mineral and bone like materials were assessed by FTIR,XRD, SEM and detection of ALP, Osteopontein and Osteocalcin amounts along the time intervals of SBF immersion(18). Chen et al, studied the bioactivity of Mg–Zn–Ca alloy when coated by silicon–calcium–phosphate (Si–CaP) on Mg–Zn–Ca alloy by IR for SBF analysis, He was found that Si–CaP coating prepared at 450 V had the best corrosion resistance, improving the biodegradation bioactivityproperties(19). Martynenko Studied bioactivity of Mg–Zn–Ca, Multipotent mesenchymal stromal cells (MMSCs) from mouse femur bone marrow were used as a cell model,they found that an extract of the alloy promoted the alkaline phosphatase activity of human mesenchymal stromal cells, which indicates osteogenic stimulation of cells(20).

Monitoring the Bioactivity behavior of MgAZ31 and Mg1Zn 0.6Ca alloys is great challenge via evaluating the amount of mineral and matrix of bone-like structure formed after immersion in SBF. Furthermore assessing the mechanical properties that varied according to biodegradation behavior and deposition of newly deposited structure along the immersion time is great importance to repair the bone defect.

Materials and Methods.

MgAZ31 alloy (available from Chemnitz University of Technology) and Mg 1Zn 0.6Ca alloy (casted at Metals Technology Department (CMRDI), Egypt) were selected in this study. A Total number of eighty rectangular rods 50 mm × 5 mm × 5 mm3 were prepared, in accordance with ASTM standard 4385:1981. The surfaces were polished mirror-like using Emery paper starting grit from 400 up to 2000 grit SiC papers. All rectangle samples were washed with 70 vol.% ethanol at room temperature, then cleaned ultrasonically in distilled water for 5 minutes and finally dried by air

drier(21). The rods were divided into two groups MgAZ31 **(Group I)** and Mg1Zn 0.06 Ca **(group II)**. The groups were subdivided according to the time intervals of biomimetic immersion in SBF (0, 2, 4, 8 weeks); n=10.The groups were;

Group IA: MgAZ31 before immersion in SBF (control).

Group IB: MgAZ31after immersion in SBF for 2 weeks.

Group IC: MgAZ31 after immersion in SBF for 4 weeks.

Group ID: MgAZ31 after immersion in SBF for 8weeks.

Group IIA: Mg1Zn 0.6Ca before immersion in SBF (control).

Group IIB: Mg1Zn 0.6Ca after immersion in SBF for 2weeks.

Group IIC: Mg1Zn 0.6Ca after immersion in SBF for 4 weeks,

Group IID: Mg1Zn 0.6Ca after immersion in SBF for 8weeks.

2.A- Qualitative analysis:

All biomimetic degraded alloy groups after different time intervals were characterized by using reflection Fourier transforms infra-red spectra (FTIR) from 400-4000 cm-1 spectra.

1. Biomimetic immersion:

The different tested groups of alloys were immersed in simulating body fluid (SBF) similar to human blood plasma; 8.0 g/l NaCl, 0.14 g/l CaCl2, 0.4 g/l KCl, 0.35 g/l NaHCO3, 1.00 g/l C6H12O (Glucose), 0.1 g/l NaH2PO4, 0.1 g/l MgCL2.6H 2O, 0.06 g/l Na2HPO42H2O, 0.06 g/l MgSO4.7H2O, at pH (7.4), at temperature (37 ± 1°C), according to (Oyane, Kim et al. 2003). The rods were suspended in a properly sealed beaker filled with 250 ml SBF solution maintained at a constant temperature of 37 ± 1°Cat pH 7.4 for different time interval 2, 4 and 8 weeks (n=10/time interval). At the end of each immersion period, the specimens were removed from the solution, gently rinsed with distilled water, and dried at room temperature.

2. Fourier transforms infrared spectroscopy (FTIR) chemical analysis:

2.B- Bioactivity testing:

Quantitative analysis for FTIR of different tested groups was employed by calculating the full width at half maximum (FWHM) i. e intensity % of reflected spectra, according to methodology described by (22). Biomimetic bioactivity of different tested groups was evaluated by calculating the quantitative amount of mineral, matrix and mineral/matrix ratio deposited on different alloys surfaces which referred to bone quality parameters according to reference values table (1). Mineral quality evaluated by phosphate contents (PO4), degree of HA crystal maturity (CO3/PO4), and degree of crystallinity (height of 563+603/height of trough between them cm-1). On the other hand, matrix was evaluated by calculating the amount of amide I. The degree of calcification (mineral to matrix ratio) was evaluated from (PO4/Amide I). The data of the deposited layer were compared with actual human bone reference data according to **Farlay, 2010**(23).

Table 1: Shows the selected parameters to assess bone quality

Parameter		IR peaks assignment	Comments
Mineral Quality	PO_4^{-3}	Integrated area of v_1, v_3 (900-1200 cm^{-1}) phosphate	Mineral content
	CO_3/ PO_4	Integrated area of sub-band at 873 cm^{-1}/ 1030 cm^{-1}	Degree of HA crystal maturity or indicates the amount of carbonate substitution for phosphate in the mineral crystals
	Crystallinity Index or Splitting Factor	Summing the heights of the 563 and 603 cm^{-1} peak and dividing this value by the height of the trough between them	Degree of HA crystallinity
Matrix Quality	Amide I	Amide I (1575-1720 cm^{-1})	Protein contents in matrix
Mineral/Matrix Ratio	PO_4^{-3}/Amide I	Integrated area of v_1, v_3 (900-1200 cm^{-1}) phosphate/amide I (1575-1720 cm^{-1})[101]	Degree of calcification

3. Flexural Strength testing:

The biomimetic immersed rods of different groups were subjected to the three-point loading fracture test by using a universal electronic Instron machine testing assembled in USA,System ID: ***(3366L8668)***. The indenter was loaded at a speed of 2 mm/min till the tested samples fractured. The flexural strength of different tested groups was calculated according to the following equation: (24).

$$R = \frac{1}{4} 3FL/ 2bh2$$

Where R is the flexural strength, F is the loading force, L is the span length, b is the width of the sample, and h is the height of the sample.

4. SEM and EDX analysis

The surface morphology of different alloys was analyzed by using SEM. The elements constituting the alloy surfaces were detected and analyzed by using Energy dispersive x-ray analysis(EDX).

5. Statistical analysis

Data of quantitative chemical analysis, flexural strength and EDX were collected and analyzed with SPSS for windows version 20 Chicago USA. A one-way ANOVA was used to compare more than two groups in unrelated samples, followed by a Tukey post hoc test. An independent sample t-test was

used to compare two groups in unrelated samples. P-value was considered significant at ≤ 0.05.

Results:

1. Fourier transforms infrared spectroscopy (FTIR) chemical analysis:

1.A- Qualitative analysis results:

The characteristic FTIR spectra for Group I was shown in **Fig (1).** The spectra revealed the presence of Mg-O, AL-O, and Zn–O and their changes after immersion in SBF at different time intervals. After the biomimetic immersion in (SBF); the spectra revealed the appearance of PO4-3(υ4), PO4-3(υ1), HPO4-2, and CO3-2 that indicated the HA deposition. The precipitation of Mg (OH)2 was detected and the amide I, CH3 and OH-group were captured.

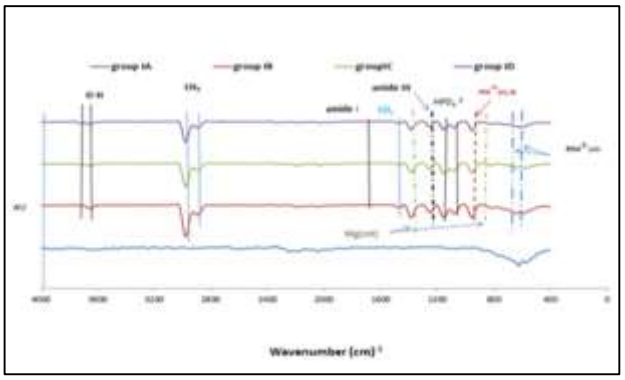

Figure 1: The characteristic FTIR spectra for Group IA, IB, IC and ID.

The characteristic FTIR spectra for group IIA is shown in **Fig (2).** The spectra revealed the presence of Mg-O, CaCO3,and Zn–O and their changes after immersion in SBF at different time intervals. After the biomimetic immersion in (SBF); the spectra revealed the appearance of PO4-3(υ4), PO4-3(υ1), HPO4-2, and CO3-2 that indicated the HA deposition. The precipitation of Mg (OH)2 was detected and the amide I, CH3 and OH-group were captured.

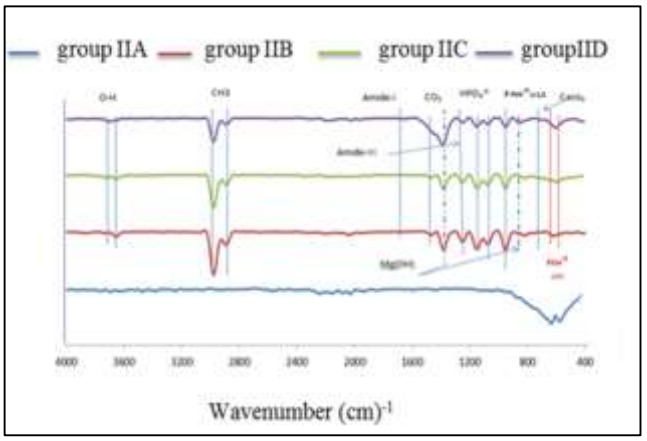

Figure 2: The characteristic FTIR spectra for group IIA, IIB, IIC and IID

1.b. Bioactivity testing:

The quantitative amount of mineral was assessed by amount of PO4, CO3/PO4 (HA crystal maturity) and the degree of HA crystallinity. The amount of PO4 (mineral amount) in normal Cancellous human bone reference was 120.79 (100%). The both groups recorded very low amount of mineral deposition when compared to reference bone. The statistical analysis of mineral amount after two weeks biomimetic immersion of group I was (0.03±0.003)0.025%) that was excessively increased after four weeks to be(0.08±0.003)(0.07%) and finally after eight weeks decreased to be(0.05±0.003)(0.04%). On other hand group II was recorded highly reduced amount of mineral. After two weeks it was 0.003±0.0002(0.0025%), and excessively increased after four weeks to be 0.02±.001(0.02%),finally reduced to be 0.01±.0005 (0.014%).The crystal maturity of normal reference Cancellous bone was 1.54 (100%).The statistical analysis of crystal maturity after two weeks from biomimetic immersion of group I was 0.04±0.003 (2.6%) and excessively increased to double value after four weeks to be 0.08±0.002 (5.2%) and finally after eight weeks reduced to 0.05±0.003 (3.3%). Whereas the crystal maturity of group II recorded excessive hugged values. After two weeks it was 1.20±0.40 (77.9%) and decreased after four weeks to be 0.83±0.26 (53.9%) and finally after eight weeks excessively increased to be 2.48±0.85(161%).

The degree of HA crystallinity of normal reference Cancellous bone was 24.9 (100%). The statistical analysis of degree of HA crystallinity after two weeks from biomimetic immersion of group IB was 1.85±0.23 (7.4) and decreased after four and eight weeks to be(1.56±0.04(6.3) and (1.84±0.02 (7.3%)respectively.Whereas the degree of HA crystallinity of group II recorded hugged values.

After two weeks it was 5.14±0.18(20.6%) and significantly decreased after four weeks to be 1.33±0.01 (5.3%) and finally after eight weeks excessively significant increased to be 16.32±0.32 (6.5%) (65.5%).

The matrix quality was evaluated according to amide I content and compared to those of normal reference Cancellous bone; (11.8a.u) (100%). The statistical analysis for amount of amide I deposited after biomimetic immersion of group I and the group II recorded non-significant statistical constant value for amide I after two, four and eight weeks, it was 0.001±0.002 (0.008%).

Mineral / matrix ratio of normal reference Cancellous bone was 10.28 (100%).The statistical analysis of the Mineral / matrix ratio after two weeks from biomimetic immersion of group I was 30.27±0.18 (257.9%). After four weeks significant increased to be 80.35±0.24 (683.8%) and finally after eight weeks decreased to be 50.39±0.30 (428.8%) **Fig (3).** Whereas the Mineral / matrix ratio of group II recorded lesser values than group I. After two weeks it was 3.39±0.33(28.9%) and significantly increased after four weeks to be 25.44±0.34.

Table 2: The statistical analysis for bone quality Parameters of group I and GroupII after immersion in SBF at different time intervals.

Parameter of bone quality		normal reference **Cancellous** bone	Group IA (MAZ31)			Group IIA (Mg1Zn0.6Ca)			p-value for each raw
			IB	IC	ID	IIB	IIC	IID	
Mineral Quality	Mineral content (PO_4)	120.79±0.45 A	0.03±0.003C (0.025%)	0.08±0.003B (0.07%)	0.05±0.003B (0.4%)	0.003±.0002D (0.0025%)	0.025±.001 C (0.02%)	0.017±.000EC (0.014%)	<0.001
	HA crystal maturity CO3/PO4	1.54±0.48 B	0.04±0.003B(2.6%)	0.08±0.002E (5.2%)	0.05±0.003E (3.3%)	1.20±0.40C (77.9%)	0.83±0.26D (53.9%)	2.48±0.85A (161%)	<0.001
	HA crystallinity	24.9±0.18 A	1.85±0.23B (7.4%)	1.56±0.04D (6.3%)	1.84±0.02 D (7.4%)	5.14±0.18C (20.6%)	1.33±0.01 E (5.3%)	16.32±0.32B (65.5%)	<0.001
Matrix quality	Amide I	10.28±0.001 A	0.001±0.002B (0.008%)	0.001±0.002B (0.008%)	0.001±0.002B (0.008%)	0.001±0.002B (0.008%)	0.001±0.002B (0.008%)	0.001±0.002B (0.008%)	<0.001
Mineral/Matrix Ratio	PO_4^{3-}/Amide	11.75±0.002E	30.3±0.18 C(257.9%)	80.35±0.24A(683.8%)	50.39±0.30B(428.85%)	3.39±0.33G(28.9%)	25.44±0.34D(216.5%)	17.76±1.58F(151.1%)	<0.001

2. Flexural strength.

The statistical analysis of the flexural strength of Group IA was (144.45±.03 MPa) that was significantly decreased after two weeks (group IB) to be (102.65±.03 MPa) then excessively decreased to the least significant value at eight weeks (group ID) (5.76±.03 MPa), On other hand the statistical analysis of the flexural strength of Group IIA was (160.56±.03 MPa) that was significant decreased after two weeks (group IIB) to be(130.67±.03 MPa)then excessively decreased with significant value at four and eight week (groupIID) (95.75±.03and 88.75±.03 MPa) respectively.

The statistical analysis for initial flexural strength of group II A was higher than group IA;(160.56±0.03and 144.45±0.03Mpa) respectively. Group II recorded the highest significant strength along the different time intervals compared to group I, as shown in **Table 3** and **Fig 3**.

Table 3: The statistical analysis of the flexural strength (Mpa) among studied groups.

	(Group I) Mg AZ 31(Mpa)	(Group II) Mg 1zn0.6ca (Mpa)
	Mean ±SD	Mean ±SD
Control (A)	144.45±0.02A	160.56±0.03A
Two weeks(B)	102.65±0.03B	130.67±0.02B
Four weeks (c)	17.86±0.03C	95.75±0.03C
Eight weeks(D)	5.76±0.03D	88.75±0.01D
p-value for each column	<0.001	<0.001

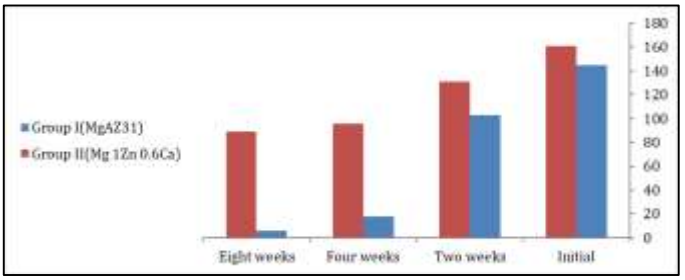

Figure 3: Histogram of the statistical analysis of the flexural strength (Mpa) among studied groups.

3. SEM and EDX examination:

The main microstructural constituents of group IA (MgAZ3l) and (Mg1Zn0.6Ca)are shown in the SEM image **Fig (4)**. The SEM image after two weeks for (group I,II) showed the presence of the protective layer of Mg (OH)2 and showed the presence of the calcium phosphate layer on alloysurface at 2weeks,8weeks.

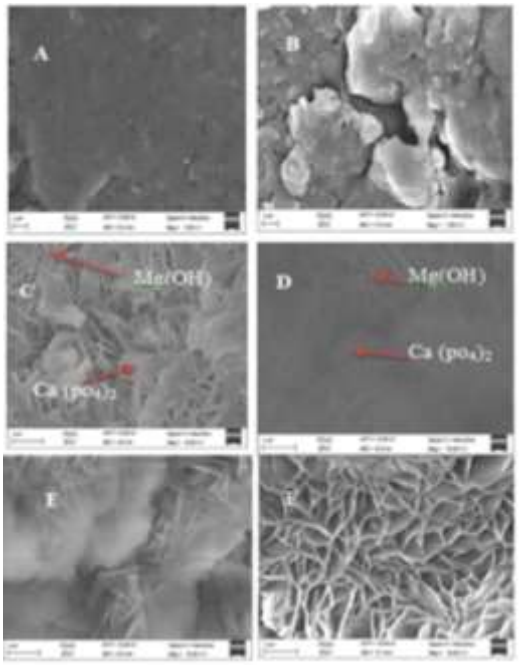

Figure 4:SEM image of the tested groups(A)for control groupI (MgAZ31),(C)for group IB,(E)for group ID, while (B) for control group II (Mg1Zn0.6Ca) ,(D)for group IIB,(F) for group IID.

EDX analysis for elements before and after biomimetic immersion for2weeks, 4weeks and 8weeks of Mg-alloys are presented in **Table 4** and **Fig (5).**

Table 4; The statistical analysis of EDX of group I and GroupII before and after immersion in SBF.

elements	Group I(Mg AZ 31)				Group II (Mg 1Zn0.6Ca)				p-value
	Control	2w	4w	8w	Control	2w	4w	8w	
Mg	94.8±0.99 B (100%)	38.54±0.03D (40.6%)	36.46±0.14 D (38.5%)	31.35±0.03E (33%)	96.3±1.41 A (100%)	45.3±0.10C (47.04%	43.82±0.17 C(45.5	43.09±0.03C (44.7%)	<0.001
Zinc	1.7±0.18A (100%)	1.2±0.03B (70.6%)	1.01±0.05B (59.4%)	0.55±0.05E(32.4)	1.79±0.19 A (100%)	0.78±0.03D (43.5%)	0.94±0.21C (52.5%)	0.32±0.03F (17.9%)	<0.001
Al	3.5±1.05A (100%	0.34±0.03B (9.7%)	0.33±0.03B (9.4%)	0.32±0.03B (9%)	0±0	0±0	0±0	0±0	<0.001
O	0±0	55.7±0.03C (100%)	57.8±0.54B (103.8%)	61.52±0.56A (110.4%)	0±0	58.6±.30B(100%)	59.2±0.19A (69.2%)	60.85±0.53A (103.8%)	<0.001
Ca	0±0	0.34±0.03F (100%)	0.55±0.12D (161.7%)	2.1±0.08A (617.6%)	1.92±0.71 B(100%)	0.35±0.04F (18%)	0.88±0.08C (45.8%)	0.43±0.03E(22.4%)	<0.001
P	0±0	0.73±0.03D (100%)	0.84±0.03C (115%)	0.65±0.03E (89%)	0±0	1.5±0.43A (100%)	0.93±0.06B (62%)	0.97±0.03B(64.7%)0	<0.001
Na	0±0	0.44±0.02A(100%)	0.054±0.02 C (12.3%)	0.14±0.04B (31.8%)	0±0	0.054±0.02 C(100%)	0.054±0.02 C(100%)	0.14±0.03B(259.3)	<0.001
Cl	0±0	0.46±0.28D	0.34±0.03E	0.78±0.02C	0±0	0.22±0.02F	0.84±0.03B	1.04±0.02A	<0.001

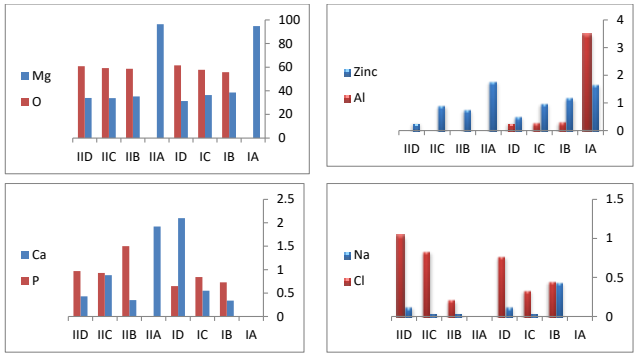

Figure 5: Elements detected on scanned studied Mg-alloy surfaces at different time intervals and control.

Discussion:

Magnesium and its alloys is now a promising regenerative alloy for biomedical Osseo induction applications. MgAZ31 and Mg1Zn 0.6Ca alloys are newly regenerative alloys(25) (12).The Osseo induction and regenerative power of both alloys were studied after immersion in SBF for eight weeks. Bioactive materials are the ability to form hydroxyapatite (HA), a calcium phosphate mineral phase similar to inorganic part of human bone on its implant surface(18). This study focused on studying the qualitative and quantitative newly formed minerals and matrix after biomimetic immersion in SBF for eight weeks and correlated to normal human bone quality.

The FTIR analysis of group IA (MgAZ31) revealed the heterogeneous surface of the alloy that formed from Mg-O, Al-O and Zn-O, **Fig (1).** The EDX analysis revealed massive loss of many elements; Mg, Zn, and Al after two weeks and other elements were detected on the surface; O, Cl, Na, Ca, and P, after the biomimetic immersion of MgAZ31 alloy in SBF. Mg, Zn, and Al elements decreased from the surface by about (60, 30, and 90%), respectively due to the oxidation of Mg and evolution of hydrogen bubbles, Table (4), and fig (5). This might be attributed to develop of electrochemical corrosion between the α-Mg matrix and the eutectic phase of MgZnAl constituents of alloy led to the depletion of Mg, Zn, and Al elements from surface and hydrogen evolution that led to more pitting corrosion, (11)(8).

In which large concentration gradients developed between the alloy surface and the SBF solution that led to local alkalization producing more OH- anions and Mg+2 cations. The protective layer of Mg (OH)2 was formed in group I after two weeks as shown in SEM **fig(4).** This explained the massive degradation of Mg ions initially (60%) that became less after four and eight weeks that was synchronized by increased in oxygen %, Table 4, fig (5). The high degradation rate of magnesium alloys in SBF might have also resulted from an aggressive attack by chloride, sulfate, phosphate, and carbonate ions, among which chloride ions have the biggest threat. Chloride ions can transform the surface Mg(OH)2 into more soluble MgCl2. Dissolution of Mg(OH)2 makes the surface more active, consequently promoting further dissolution of magnesium.

$Mg \leftrightarrow Mg^{+2}+2e-$ (1)

$2H_2O+2e- \rightarrow H_2\uparrow+2OH-$ (2)

$Mg^{2+}+2OH- \rightarrow Mg(OH)2$ (3)

$Mg(OH)_2 \rightarrow MgCl_2(soluble)+2OH-$ (4)

The high degradation of Mg ions increased the concentration of magnesium ions in SBF. Furthermore, Mg $(OH)_2$ considered as a nuclei that allowed a magnesium-containing calcium phosphate precipitated from the SBF on the surface of the magnesium implant as shown in SEM, Fig 5, according to the following reaction:

$Mg^{2+} + Ca^{2+} + HPO4^{-} \rightarrow MgxCay(PO4)z$ (5)

$10\ Ca^{2+} + 6PO4^{3-} + 2OH- \rightarrow Ca\ 10(PO4)6(OH)2$(6)

It was observed right shifting of MgO peaks from 588 to 582 cm-1 and left shifting of 624 to 646 cm-1 means formation of PO4 and OH attached to PO4 which indicated the HA crystal formation, **Fig (1)** The high Ca^{2+} and Mg^{2+} contents in this degradation layer in turn accelerate the deposition of biological calcium phosphate (hydroxyapatite crystals HA) on the surface. Furthermore, time immersion enhanced more mineral deposition; PO4, HCO3 and Mg (OH) and HA formation due to right shift of HPO4-2 group to be 1090, and 1150 cm-1, **Fig(1)**. It was observed that; the degradation rate of MgAZ31decreased after four and eight weeks compared with two weeks this might be due to the formation of protective passive layer of $Mg(OH)_2$,calcium phosphate compound and HA crystals, as shown in SEM, **Fig4 C** , in agreement with (2)(26)(11).

Group II alloy contains calcium as one of alloying elements to improve the biocompatibility and Osseo inductivity more than aluminum element(27). In which the FTIR analysis revealed the presence of characteristic bands of MgO, ZnO, and CaCO3,**Fig (2).** The EDX analysis revealed loss of many elements; Mg, Zn, and Ca after two weeks when compared with group IB and other elements were detected on the surface; O, Cl, Na, and P, after the biomimetic immersion of Mg1Zn0.6Ca alloy in SBF. Mg, Zn, and Ca elements decreased from the surface by about (53, 57, and 82%), respectively due to the oxidation of Mg and evolution of hydrogen bubbles according to equation 2. The Increased in loss of Zn and Ca element might be attributed to presence of Zn in eutectic phases CaMgZn and MgZn.Both of eutectic phases form anodic part in electromotive circuit while alpha Mg phase is the cathode part that increased galvanic corrosion and enhance surface degradation of the alloy. Adding to galvanic corrosion the pitting corrosion occurred led to hydrogen evolution that led to more pitting corrosion this led to excessive loss of Zn and Ca in agreement with (10).

Pitting and galvanic corrosion decreased after formation of the protective layer of Mg (OH) 2 whereas the Ftir spectra revealed the appearance of Mg (OH)2 at two bands at 800cm-1 and 1398 cm -1 shown in **Fig (1)**and SEM**Fig (4)**as in above equation3 (6) .

Adding to protective Mg(oH)2 formation it was observed thatright shifting of MgO peaks from 590 to 646 and left shifting of 526 to 636 cm means formation of PO4 and OH attached to PO4 which indicated the HA crystal formation, **Fig(2).** The high Ca^{2+} and Mg^{2+} contents in this degradation layer in turn accelerate the deposition of biological calcium phosphate (hydroxyapatite crystals HA) on the surface. Furthermore, time immersion enhanced more mineral deposition; PO4, HCO3 and Mg (OH) and HA formation due to right shift of HPO4-2 group to be 1087, and 1160 cm-1, **Fig (1).** It was observed that the amount of Mg ions after 4weeks was non-significant with 8weeks; this mean further more degradation of Mg ion was suppressed. this might be due to more the formation of protective passive layer of $Mg(OH)_2$,calcium phosphate compound and HA crystals, in agreement with(6)(27).

The Osseo bioactivity of the studied alloys were quantitatively measured by calculating the amount of PO4, CO3/PO4 (HA crystal maturity), the degree of HA crystallinity, amide I and PO4 / amide I that formed after SBF immersion to indicate the quality of bone like structure (23).

HA crystal maturity (CO3/PO4) and degree of HA crystallinity in group I was 2.6% and 7.4% from normal Cancellous bone after two weeks that increased after four weeks to be 5.2% and 6.3% whereas after eight weeks decreased again to be 3.3% and 7.4% from normal Cancellous bone. This indicated the process of bone formation; first deposition of bone after two weeks, then followed by furthermore deposition after four weeks and remodeling of formed bone like material after eight weeks. This represented poor developed mineral quality formed with type of alloy. This might be attributed to rapid degradation of MgAZ31 that led to acidic condition in the media and didn't allow the HA crystal to be well matured along, the matrix quality was poorly developed. Amide I was 0.008% from natural normal bone along all time. The degree of calcification (PO4 / amide I) was 427% after eight weeks. This might be due to the in-vitro

condition of study that depended only on SBF without considering the other vital environmental factors (protein derived; hormones, vital cells and enzymes). C=O and CH groups were deposited from glucose that constituted in SBF consequently led to undeveloped amide I and immature matrix-like structure. The bone formed was more resemble the callus stage formation after bone surgery which was take 2 weeks in human body, in agreement with (28).

HA crystal maturity (CO3/PO4) and degree of HA crystallinity in group II was 68% and 20.6% from normal Cancellous bone after two weeks that decreased after four weeks to be 53.9% and 5.3% whereas after eight weeks increased again to be 161% and 65.5% from normal Cancellous bone. The mineral quality of Mg1Zn 0.6Ca (group II) was more mature and well developed than MgAZ31 (group I). This might be due to the presence of calcium in the constitution of alloy. Calcium act as nuclei of HA crystal formation and enhanced the more adhesion of crystal to the surface of Mg-implant, (6). Amide I was 0.008% from natural normal bone along all time as in group I, this attributed to the same cause was mentioned above with group I. The degree of calcification (PO4 / amide I) was 28.7, 216.5 and 151% after two, four and eight weeks, respectively. The degree of calcification was more qualified than group I. This might be attributed to the rate of mineral deposition and resorption, first mineral deposited with balanced amide I, then mineral and crystal resorption that led to more amide I interlacing with mineral and finally more mineral deposition.Worth mentioning the crystal maturity (CO3/PO4) was 161%, that means CO3 was substituted the PO4 in the HA crystals, this might be attributed to less Calcium concentration on the alloy surface that enhanced the more CO3 ions deposition due to degradation of alloy surface, as occurred in Osteoporosis(29). The remodeling of mineral and matrix with Mg1Zn0.6Ca alloy was more resembled human body remodeling (mineral deposition, resorption and finally deposition (28).

The statistical analysis for initial flexural strength of group IIA was higher than group IA; (160.56±0.03and 144.45±0.03Mpa), respectively. This might be due to the composition of Mg1Zn0.6Ca. In which Zinc formed the solution hardening effect with magnesium alloy. In addition to that calcium act as grain refiners and formed precipitation hardening of the Ca2Mg5Zn13 phase that enhanced the strengthening effect of Mg-alloy(30) (14),also Ca content of 0.6 wt % exhibited higher bending and compressive strengths (31).

While MgAZ31 (group I) composed from $Mg_{17}Al_{12}$ precipitation hardening phase and MgZn eutectic alloy that led to a more brittle nature of the alloy and catastrophic failure(32). MgAZ31 revealed marked decrease in the strength with furthermore immersion in SBF as shown in **table (3)** and **fig (3).** This might be attributed to the rapid degradation rate of MgAZ31 compared with Mg1Z0.6Ca alloy. Where the EDX analysis revealed massive loss of many elements; Mg, Zn, and Al after two weeks, that increased more until eight weeks due to pitting, micro-galvanic, and localized corrosion.

While the EDX analysis of group II revealed less loss of the amount of many elements; Mg, Zn, and Ca than group I along the different time of immersion, **Table (3)**and**Fig(5).** The Mg1Z0.6Ca alloy revealed less degradation power in addition to furthermore qualified minerals deposited on the alloy surface that enhanced the alloy strength(33).

Conclusions:

Under limitation of this study the following finding can be drawn:

Mg1Zn0.6Ca alloy is a promising alloy for bioactive regenerative bone substitution.

-Mg1Zn 0.6Ca enhanced the deposition of mature HA with better crystallinity and rational degree of calcification near normal bone in composition. More time of immersion in SBF is needed for more assessment.

-Mg1Zn0.6Ca alloy allowed the formation of HA crystal after four weeks

-Immersion of the Mg-alloy in SBF encouraged deposition of minerals with different quality rather than the matrix.

-Flexural strength decreased along the time although the mineral deposition. AZ31 revealed the least flexural strength at all immersion time and catastrophic fracture (brittle fracture). Whereas Mg1Zn0.6Ca alloy revealed rational flexural strength which is superior than AZ31.

List of Abbreviations:

FTIR: Fourier transforms infrared spectroscopy **SBF:** simulating body fluid; **XRD:** X-ray diffraction analysis; **SEM:** scanning electron microscope; **EDX:** Energy dispersive x-ray analysis;**(CMRDI):**central

metallurgical research and development institute; **HA:**Hydroxyapatite.

Declarations

- Ethics approval and consent to participate

Not applicable

- Consent for publication

Not applicable

- Availability of data and materials

The authors announce that the data supporting the results of this study are existing within the article.

- Competing interests

No competing interests.

- Funding

This research did not receive any specific grant from backing supports in thePublic, commercial, or not-for-profit sectors.

Authors' contributions

R.S performed the whole methodology steps, helped in analysis of data and writing the manuscript and publication process. **H A. S.** performed the study design,analysis of data and helped in writing the results,discussion and manuscript.**M.S,** helped in polishing and preparing the samples and the biodegradation test in her lab in (CMRDI) and XRD analysis. **H.M.**supplied (Mg1Zn0.6Ca) alloy.

Acknowledgements

Prof. Dr.Thomas Lampke supplied(MgAZ31) alloy.

Professorship Materials and Surface Engineering. Chemnitz University of Technology (Erfenschlager Str. 73 | Room B112 D-09125 Chemnitz Germany).

REFERENCES

1. **Shalaby H, khairy N, Moussa M.** Osteoconductivity of Two Novel Biodegradable Magnesium Alloys (ZK30A&ZK10A) for Repairing Bone Defect in Dogs. Egypt Dent J. 2018;64(3):2171–82.
2. **Li L, Zhang M, Li Y, Zhao J, Qin L, Lai Y.** Corrosion and biocompatibility improvement of magnesium-based alloys as bone implant materials : a review. 2017;129–37.
3. **Chen Y, Dou J, Yu H, Chen C.** Degradable magnesium-based alloys for biomedical applications : The role of critical alloying elements. 2019;
4. **Bai H, He X, Ding P, Chen M.** Fabrication , microstructure , and properties of a biodegradable Mg-Zn-Ca clip. 2018;1741–9.
5. **Tong LB, Zheng MY, Xu SW, Kamado S, Du YZ, Hu XS, et al.** Effect of Mn addition on microstructure, texture and mechanical properties of Mg-Zn-Ca alloy. Mater Sci Eng A. 2011;528(10–11):3741–7.
6. **Kaviani M, Ebrahimi GR, Ezatpour HR.** Improving the mechanical properties and biocorrosion resistance of extruded Mg-Zn-Ca-Mn alloy through hot deformation. Mater Chem Phys [Internet]. 2019;234(May):245–58. Available from: https://doi.org/10.1016/j.matchemphys.2019.06.010
7. **Esmaily M, Shahabi-Navid M, Svensson JE, Halvarsson M, Nyborg L, Cao Y, et al.** Influence of temperature on the atmospheric corrosion of the Mg-Al alloy AM50. Corros Sci [Internet]. 2015;90:420–33. Available from: http://dx.doi.org/10.1016/j.corsci.2014.10.040
8. **Zhang F, Zhang C, Zeng R, Song L, Guo L, Huang X.** Corrosion resistance of the superhydrophobic Mg(OH)2/Mg-Al layered double hydroxide coatings on magnesium alloys. Metals (Basel). 2016;6(4):1–14.
9. **Murni NS, Dambatta MS, Yeap SK, Froemming GRA, Hermawan H.** Cytotoxicity evaluation of biodegradable Zn-3Mg alloy toward normal human osteoblast cells. Mater Sci Eng C. 2015;49:560–6.
10. **Jiang P, Blawert C, Zheludkevich ML.** The Corrosion Performance and Mechanical Properties of Mg-Zn Based Alloys — A Review. 2020;92–158.
11. **Mena-morcillo E, Veleva L.** Degradation of AZ31 and AZ91 magnesium alloys in different physiological media : Effect of surface layer stability on electrochemical behaviour. J Magnes Alloy [Internet]. 2020;(xxxx). Available from: https://doi.org/10.1016/j.jma.2020.02.014
12. **Liu C, Ren Z, Xu Y, Pang S, Zhao X, Zhao Y.** Biodegradable Magnesium Alloys Developed as Bone Repair Materials : A Review. 2018;2018.
13. **Zhang B, Wang Y, Geng L, Lu C.** Effects of calcium on texture and mechanical properties of hot-extruded Mg-Zn-Ca alloys. Mater Sci Eng A [Internet]. 2012;539:56–60. Available from: http://dx.doi.org/10.1016/j.msea.2012.01.030
14. **Maleki E, Shahri F, Emamy M.** Microstructure and Tensile Properties of Mg–5Zn Alloy Containing Ca. Met Mater Int [Internet]. 2021;27(6):1565–77. Available from: https://doi.org/10.1007/s12540-019-00530-w
15. **Li H, Qin S, Ma Y, Wang J, Liu Y, Zhang J.** Effects of Zn content on the microstructure and the mechanical and corrosion properties of as-cast low-alloyed Mg – Zn – Ca alloys. 2018;25(7):800–9.
16. **Du YZ, Qiao XG, Zheng MY, Wang DB, Wu K, Golovin IS.** Effect of microalloying with Ca on the microstructure and mechanical properties of Mg-6 mass%Zn alloys. Mater Des. 2016;98:285–93.
17. **Lin G, Chen M, Zhao Y, Sasikumar Y, Tie D.** The Mechanical Properties and Corrosion Resistance of Magnesium Alloys with Different Alloying Elements for Bone Repair. 2018;
18. **Sunil BR, Kumar AA, Sampath Kumar TS, Chakkingal U.** Role of biomineralization on the degradation of fine grained AZ31 magnesium alloy processed by groove pressing. Mater Sci Eng C [Internet]. 2013;33(3):1607–15. Available from: http://dx.doi.org/10.1016/j.msec.2012.12.095
19. **Chen C, Dou J, Zhao Y, Lu L, Gu G, Yu H, et al.** Effect of the second-step voltages on the structural and corrosion properties of silicon – calcium – phosphate (Si – CaP) coatings on Mg – Zn – Ca alloy. 2018;
20. **Martynenko NS, Anisimova NY, Rybalchenko O V., Kiselevskiy M V., Rybalchenko G, Straumal B, et al.** Rationale for processing of a mg-zn-ca alloy by equal-channel angular pressing for use in biodegradable implants for osteoreconstruction. Crystals. 2021;11(11).
21. **Rad HRB, Idris MH, Kadir MRA, Farahany S.** Microstructure analysis and corrosion behavior of biodegradable Mg-Ca implant alloys. Mater Des [Internet]. 2012;33(1):88–97. Available from: http://dx.doi.org/10.1016/j.matdes.2011.06.057
22. **Mingo B, Guo Y, Leiva-Garcia R, Connolly BJ, Matthews A, Yerokhin A.** Smart Functionalization of Ceramic-Coated AZ31 Magnesium Alloy. ACS Appl Mater Interfaces. 2020;12(27):30833–46.
23. **Farlay D, Panczer G, Rey C, Delmas PD, Boivin G.** Mineral maturity and crystallinity index are distinct characteristics of bone mineral. J Bone Miner Metab. 2010;28(4):433–45.
24. **Hu Y, Guo X, Qiao Y, Wang X, Lin Q.** Preparation of medical Mg–Zn alloys and the effect of different zinc contents on the alloy. J Mater Sci Mater Med. 2022;33(1).
25. **Li Y, Pan Q, Xu J, He X, Li HA, Oldridge DA, et al.** Overview of methods for enhancing bone regeneration in distraction osteogenesis: Potential roles of biometals. J Orthop Transl. 2021;27(November 2020):110–8.
26. **Wang C, Wu L, Xue F, Ma R, Hao X, Dong J, et al. SC.** J Mater Sci Technol [Internet]. 2018;(2010). Available from: http://dx.doi.org/10.1016/j.jmst.2018.01.015
27. **Li Z, Gu X, Lou S, Zheng Y.** The development of binary Mg e Ca alloys for use as biodegradable materials within bone. 2008;29:1329–44.
28. **Ahmed R, Law AWL, Cheung TW, Lau C.** Raman spectroscopy of bone composition during healing of subcritical calvarial defects. Biomed Opt Express. 2018;9(4):1704.
29. **Glimcher MJ.** The Nature of the Mineral Phase in Bone: Biological and Clinical Implications [Internet]. Metabolic Bone Disease and Clinically Related Disorders. Woodhead Publishing Limited; 1998. 23-52e p. Available from: http://dx.doi.org/10.1016/B978-012068700-8/50003-

7
30. **Lu Y, Bradshaw AR, Chiu YL, Jones IP.** Effects of secondary phase and grain size on the corrosion of biodegradable Mg-Zn-Ca alloys. Mater Sci Eng C. 2015;48:480–6.
31. **Zhang CZ, Zhu SJ, Wang LG, Guo RM, Yue GC, Guan SK.** Microstructures and degradation mechanism in simulated body fluid of biomedical Mg-Zn-Ca alloy processed by high pressure torsion. 2016;
32. **Papenberg NP, Gneiger S, Weißensteiner I, Uggowitzer PJ, Pogatscher S.** Mg-Alloys for Forging Applications — A Review. 2020;1–61.
33. **Sun Y, Zhang B, Wang Y, Geng L, Jiao X.** Preparation and characterization of a new biomedical Mg-Zn-Ca alloy. Mater Des [Internet]. 2012;34:58–64. Available from: http://dx.doi.org/10.1016/j.matdes.2011.07.058